

Environmental And Economic Optimization For Transmission Power Networks With Facts And Renewable Power Sources Using Artemisinin Optimization Algorithm

Tuan Anh Nguyen¹, Le Chi Kien², Hai Van Tran^{3*}, Phu Trieu Ha⁴, Ly Huu Pham⁵, Thang Trung Nguyen⁵

¹ PhD. Student, Faculty of Electrical and Electronics Engineering, Ho Chi Minh City University of Technology and Education, Ho Chi Minh City, Vietnam,

² Faculty of Electrical and Electronics Engineering, Ho Chi Minh City University of Technology and Education, Ho Chi Minh City, Vietnam; tuanna.ncs@hcmute.edu.vn; kienlc@hcmute.edu.vn

³ Faculty of Electrical and Electronics Engineering, Ho Chi Minh City University of Industry and Trade, Ho Chi Minh City, Vietnam; haitv@huit.edu.vn

⁴ Faculty of Engineering and Technology, Saigon University, Ho Chi Minh City, Vietnam; phu.ht@sgu.edu.vn

⁵ Power System Optimization Research Group, Faculty of Electrical and Electronics Engineering, Ton Duc Thang University, Ho Chi Minh City, Vietnam; phamhuuly@tdtu.edu.vn; nguyentrungthang@tdtu.edu.vn

*Corresponding Author: haitv@huit.edu.vn

Abstract

The study applies the Artemisinin Optimization algorithm (AO) and Tunicate Swarm Algorithm (TSA) to optimally place wind power plant (WPP) and flexible alternating current transmission system (FACTS) in an IEEE 30-bus transmission power grid (TPG). Four study cases are implemented by using AO and TSA, including Case 1) one 15-MW WPP; Case 2) one 15-MW WPP and one Thyristor Controlled Series Compensator (TCSC); Case 3) One 15-MW WPP and one Static Var Compensator (SVC); and Case 4) One 15-MW WPP, one TCSC and one SVC. AO is better than TSA for the four cases, reaching smaller power loss and better 50 trial runs for each case. In addition, AO can escape the local zones and find better solutions than TSA; meanwhile, TSA falls into local zones. The loss of AO is smaller than that of TSA by 4.7%, 3.5%, 4.27%, and 4.87% for the four cases, respectively. The two algorithms can find the smallest loss for Case 4 and the highest loss for Case 1 among the four cases. In addition, Case 4 reduces emission by 1.99, 2.01, 0.92, and 19.68 kg compared to Case 1, Case 2, Case 3, and Base case. For a 20-year period, the system can save 344,829.92 dollars for environmental purpose. So, the use of both TCSC and SVC is better than the cases without them or only one of them, and AO is suitable for placing the WPP and FACTS devices in the TPG.

Keywords: Wind power plant; FACTS; power loss; Artemisinin Optimization algorithm; Tunicate Swarm Algorithm

I. INTRODUCTION

Power systems have three popular parts, including power sources, transmission and distribution networks, and electric loads [1]. Among the four parts, power sources (generators and transformers) and transmission networks are two major parts of transmission power grids [2]. The costs for producing electricity and energy loss in the grids are significant and account for a high number of the total costs of the power system. So, the study focuses on the total costs of electric generation and energy loss in the transmission grids. Transmission lines are very important in transmission power grids because they are supplied by power plants and provide electricity to distribution power networks. When the lines can operate effectively and stably, other distribution grids can work well [3]. Researchers were concerned about optimal power flow (OPF) problems in the transmission networks. The original OPF problem was about the optimization of control parameters of existing devices in the power systems, such as transformers, lines, capacitors, and generation of power plants to reduce the electric generation fuel cost and emission of thermal power plants (ThPPs), and improve the voltage of loads [4]. When renewable power sources were applied popularly in power systems, the OPF problem combined the power sources [5]. The optimal placement of wind power plants [6], solar power plants [7], both solar and wind power plants (WPPs) [8] was proposed, which led to problems with transmission, such as overloading status for lines. The

installation of renewable power sources can reduce the generation of other existing power plants, reduce the energy cost and energy loss cost [9], improve the voltage of loads, reduce the loading of lines, and stabilize the frequency of grids [10]. The Newton-Graphson method was one of the most popular methods for solving the classical OPF problem [11], but it cannot be applied to more complicated problems regarding renewable power sources in the grids. In the new problem, the solutions that were obtained had to reach allowable values for all devices in the grids. The combination of modern metaheuristic algorithms and Gaussidel/Newton-Graphson was proposed for the problem [12-14], where the Genetic algorithm [12], Cuckoo search algorithm [13], and Jellyfish search algorithm (JSA) [14] were the modern metaheuristic algorithm. As FACTS components were applied to power systems, the system's effectiveness increased. Namely, the loss is decreased, and the voltage is improved significantly. The FACTS components can supply and absorb reactive power, change the parameters of transmission lines, control the voltage magnitude and angle at nodes, etc. The FACTS components consist of TCSC [15], SVC [16], static synchronous compensator (STATCOM) [17], and the combination of SVC and TCSC [18]. The study applies Artemisinin Optimization algorithm (AO) [19] and Tunicate Swarm Algorithm (TSA) [20] to optimize the placement of one 15-MW wind power plant, one TCSC and one SVC in the IEEE 33-node transmission power grid. The objective is to reduce the total power loss on all transmission lines. The contributions of the study are summarized as follows:

- Find the most suitable location for installing one 15-MW WPP, one TCSC and one SVC to reach the smallest power loss.
- Compare the results of four cases, including 1) installation of one WPP, 2) one WPP and one TCSC; 3) one WPP and one TCSC; 4) one WPP, one TCSC and one SVC.
- Improve the voltage profile of the transmission power grid.

II. Problem Description

2.1. Objective functions

Transmission power grids transmit high power from power plants to loads via transmission lines. So, the total power losses on all the transmission line is very high, leading to a high energy loss. So, the study minimizes the total power losses on transmission lines when power systems are working. The objective function is expressed as follows:

$$\text{Reduce } P_{\text{Loss}} = \sum_{j=1}^{N_{\text{Node}}} \sum_{i=1; i \neq j}^{N_{\text{Node}}} CD_{ji} \cdot (U_j^2 + U_i^2 - 2 \cdot U_j \cdot U_i \cdot \cos \varphi_{ji}) \quad (\text{MW}) \quad (1)$$

where, P_{Loss} is the total active power losses on all transmission lines; φ_{ji} is the deviation of angle phases between node j and node i and it is calculated by using $\varphi_{ji} = \varphi_j - \varphi_i$, where φ_j and φ_i are the angle of voltage at buses i and j ; U_j and U_i are the voltage of buses j and i ; N_{Node} is the number of nodes; CD_{ji} is the conductance of the transmission line ij .

In addition, the study also consider the emission cost reduction as an objective function, which is shown as follows:

$$\text{Reduce Cost}_E = \text{Pri}_E \cdot (C_{e_t} \cdot P_t^2 + B_{e_t} \cdot P_t + A_{e_t} + D_{e_t} \cdot \text{Exp}(E_{e_t} \cdot P_t)) \quad (\$) \quad (2)$$

where, Pri_E is the average emission price in \$/ton; P_t is the power of the t th TGU; and A_{e_t} , B_{e_t} , C_{e_t} , D_{e_t} and E_{e_t} are emission parameters of the t th TGU.

2.2. The model of TCSC and SVC

TCSC and SVC are two popular types of FACTS. TCSC can change the parameter of lines and SVC can change the voltage of node, provide or absorb the reactive power of load. The model of TCSC in a transmission line is presented in Figure 1 [21].

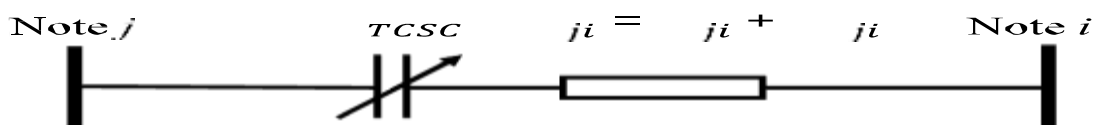


Figure 1. A transmission line with TCSC

After installing TCSC, the line has the reactance as follows:

$$X'_{ji} = X_{ji} \pm X_{\text{TCSC}} \quad (3)$$

X_{ji} and X'_{ji} are the reactance of the line ji before and after installing TCSC; and X_{TCSC} is the TCSC reactance. For a power system with more than one TCSC, each TCSC must satisfy the following

constraint:

$$X_{TCSC,h}^{Min} \leq X_{TCSC,h} \leq X_{TCSC,h}^{Max} ; h = 1, \dots, N_{TCSC} \quad (4)$$

SVC devices can inject or absorb the reactive power at a bus where it is located. SVC devices have capacitors for generating reactive power and inductors to consume the reactive power. The value of the injected or absorbed reactive power is dependent on the angle of thyristors. A typical SVC at a bus is presented in Figure 2 [22].

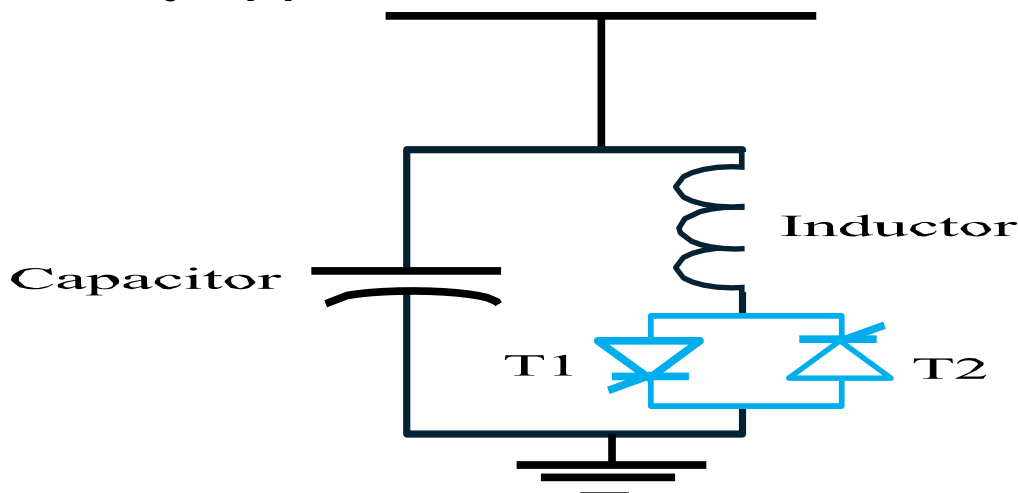


Figure 2. The structure of SVC

During the operation, SVC must satisfy its limitations as follows [22]:

$$Q_{SVC,k}^{Min} \leq Q_{SVC,k} \leq Q_{SVC,k}^{Max} ; k = 1, \dots, N_{SVC} \quad (5)$$

where $Q_{SVC,k}$, $Q_{SVC,k}^{Min}$ and $Q_{SVC,k}^{Max}$ are the real, minimum and maximum reactive power generation of the k th SVC at node j ; N_{SVC} is the number of installed SVC in the considered system.

2.3. Constraints of OPF problem with TCSC

Equality constraint: The transmission power grid has two major factors, frequency and voltage in the power quality. Normally, when the frequency and voltage are within their allowable limits, the reactive and active power equality constraints must satisfy the following formulas [23]:

$$Q_j + Q_{SVC,j} - Q_{Loadj} = U_j \sum_{i=1}^{N_{Node}} U_i \left[\begin{matrix} CD_{ji}^{TCSC} \cdot \cos(\varphi_{ji}) \\ -ST_{ji}^{TCSC} \cdot \sin(\varphi_{ji}) \end{matrix} \right] \quad (6)$$

$$P_j - P_{Loadj} = U_j \sum_{i=1}^{N_{Node}} U_i \left[\begin{matrix} CD_{ji}^{TCSC} \cdot \cos(\varphi_{ji}) \\ +ST_{ji}^{TCSC} \cdot \sin(\varphi_{ji}) \end{matrix} \right] \quad (7)$$

where Q_j and P_j are reactive and active power provide by a TGU at the j th node; Q_{Loadj} and P_{Loadj} are reactive and active power requested by loads at the j th node; and $Q_{SVC,j}$ is the generation supplied by SVC at the j th node; CD_{ji}^{TCSC} and ST_{ji}^{TCSC} are the conductance and susceptance of the line with TCSC [23].

Inequality constraints: In addition to the equality constraints above, the transmission grid must satisfy the allowable limits of electric components, such as power sources, loads, transformers, and transmission lines as follows.

$$P_t^{Min} \leq P_t \leq P_t^{Max} \quad (8)$$

$$Q_t^{Min} \leq Q_t \leq Q_t^{Max} \quad (9)$$

$$U_{Load}^{Min} \leq U_{Loadj} \leq U_{Load}^{Max} ; j = 1, \dots, N_{Node} \quad (10)$$

$$U_G^{Min} \leq U_G \leq U_G^{Max} ; n = 1, \dots, N_{TGS} \quad (11)$$

$$Tap_{Trs}^{Min} \leq Tap_{Trs,f} \leq Tap_{Trs}^{Max} ; f = 1, \dots, N_{Trs} \quad (12)$$

$$\max(|S_{ji}|, |S_{ij}|) \leq S_{ji}^{Max} \quad (13)$$

where P_t^{Min} and P_t^{Max} , and Q_t^{Min} and Q_t^{Max} are the minimum and maximum active and reactive power of the t th TGU; U_{Load}^{Min} and U_{Load}^{Max} are the minimum and maximum values of voltage for stable operation; Tap_{Trs}^{Min} and Tap_{Trs}^{Max} are the minimum and maximum tap values of transformers; and S_{ji}^{Max} and S_{ij} are the

maximum and operating apparent power of line j_i .

III. Artemisinin Optimization Algorithm

3.1. The first New solution generation

AOA use two methods for update new solutions in the first phase based on the comparison between a random number and 0.5. It means that the probability of 50% for each method is applied to produce new solutions. The two methods are included in the following formula:

$$\text{Solution}_x^{\text{new},1} = \begin{cases} \text{Solution}_x + F_1 \cdot \text{Solution}_x \cdot (-1)^t, & \text{if } P_{\text{rand}} \leq 0.5 \\ \text{Solution}_x + F_1 \cdot \text{Solution}_{\text{GBest}} \cdot (-1)^t, & \text{else} \end{cases} ; x = 1, \dots, N_{\text{sol}} \quad (14)$$

where, $\text{Solution}_x^{\text{new},1}$ and Solution_x are, respectively, the x th new and old solutions in the first generation; F_1 is the diffusion parameter; P_{rand} is a random number within 1 and 0; $\text{Solution}_{\text{GBest}}$ is the best solution of all obtained solutions; and N_{sol} is the number of solutions in the population or the population size.

3.2. The second new solution generation

This stage focuses on completely eradicating any remaining malaria parasites after the initial, widespread treatment of the first stage. While the first stage targets the parasite population broadly, this second stage targets smaller, localized areas where residual parasites might persist. The following model represents this localized eradication strategy.

$$\text{Solution}_x^{\text{new},2} = \text{Solution}_{\text{rd1}} + AP \cdot (\text{Solution}_{\text{rd2}} - \text{Solution}_{\text{rd3}}) \quad (15)$$

where, $\text{Solution}_x^{\text{new},2}$ is the x th new solution in the second phase; $\text{Solution}_{\text{rd1}}$, $\text{Solution}_{\text{rd2}}$, and

$\text{Solution}_{\text{rd3}}$ are the solutions taken randomly from the current population. and AP is the scale parameter within 0.1 and 0.6.

3.3. The post consolidation

The post consolidation is applied to reduce the malaria parasite recurrence after implementing Phase 1 and Phase 2. the kept solutions can be the old solutions or the best solution based on the comparisons between a random factor and 0.05 or 0.2 as follows.

$$\text{Solution}_x^{\text{new},3} = \begin{cases} \text{Solution}_x, & P_{\text{rand}} < 0.05 \\ \text{Solution}_{\text{GBest}}, & P_{\text{rand}} > 0.2 \end{cases} \quad (16)$$

The new solution generation methods using Phase 1 or Phase 2 is selected by comparing the iteration-based parameter- F_{iter} and a random value within 0 and 1. F_{iter} is obtained by:

$$F_{\text{iter}} = 1 - \frac{N_{\text{CI}}^{1/6}}{N_{\text{MaxI}}^{1/6}} \quad (17)$$

where RF is the reference factor; N_{CI} and N_{MaxI} are the current and maximum iteration number.

IV. NUMERICAL RESULTS

4.1. Studied system and simulation cases

In the study, TSA and AO are implemented for the IEEE 30-bus transmission power system to optimally place one 15-MW wind power plant, one TCSC, and one SVC so that the total power loss is minimal. The system's single-line diagram is plotted in Figure 3, and data are taken from [24]. The information on four study cases, population settings, and iteration numbers are given in Table 1. The emission functions of thermal power plants are reported in Table 2 [25]. The emission price is selected to be \$100 per ton.

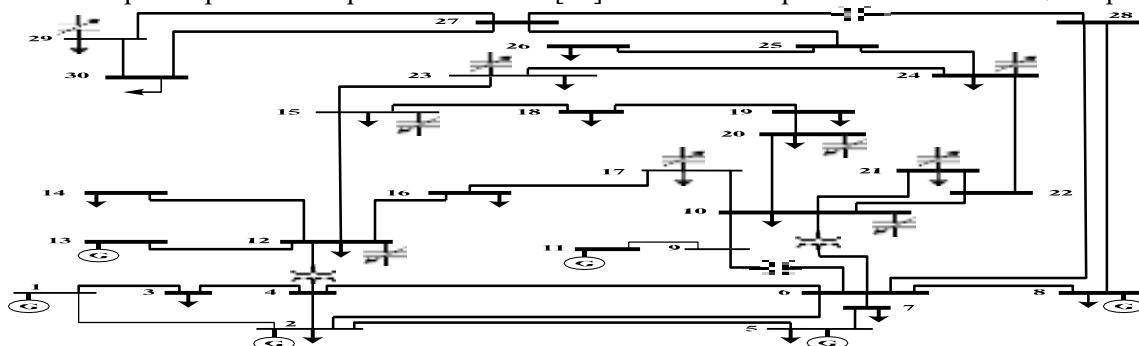


Figure 3. The IEEE 30-node system

Table 1. Description of study cases

Study case	Description of optimal placement	N_{Sol} , N_{MaxI}
1	One 15-MW WPP	100, 300
2	One 15-MW WPP and one TCSC	100, 500
3	One 15-MW WPP and one SVC	100, 500
4	One 15-MW WPP, one TCSC and one SVC	100, 700

To reach the optimal solution, TSA and AO are run for 50 trials on Matlab software with version 2018b. The simulations are executed on a personal computer with a 2.4 GHz processor and an 8-GB RAM.

Table 2. Emission parameters of TGUs

TGU	$Ae_t(\times 10^{-3})$	$Be_t(\times 10^{-3})$	$Ce_t(\times 10^{-6})$	$De_t(\times 10^{-3})$	$Ee_t(\times 10^{-3})$
1	40.91	0.5554	6.49	0.2	28.57
2	25.43	0.6047	5.638	0.5	33.33
3	42.58	0.5094	4.586	0.001	80
4	53.26	0.3550	3.38	2.0	20
5	42.58	0.5094	4.586	0.001	80
6	61.31	0.5555	5.151	1.0	66.67

4.2. Comparisons of TSA and AO

For each study case, each algorithm is run 50 times to find the power loss. The 50 power loss values are ranked from the smallest to the highest and plotted in Figures 4-7. In each figure, the first point shows the minimum loss, and the last point shows the maximum loss. AO reaches a better first point and last point than TSA. In addition, AO can reach a smaller value of power loss for 50 times. So, AO is more effective than TSA.

Figure 4. Power loss of 50 trials for Case 1

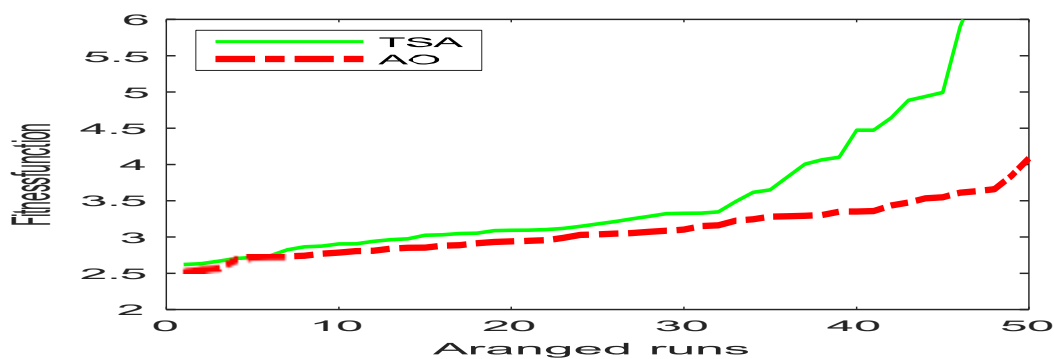
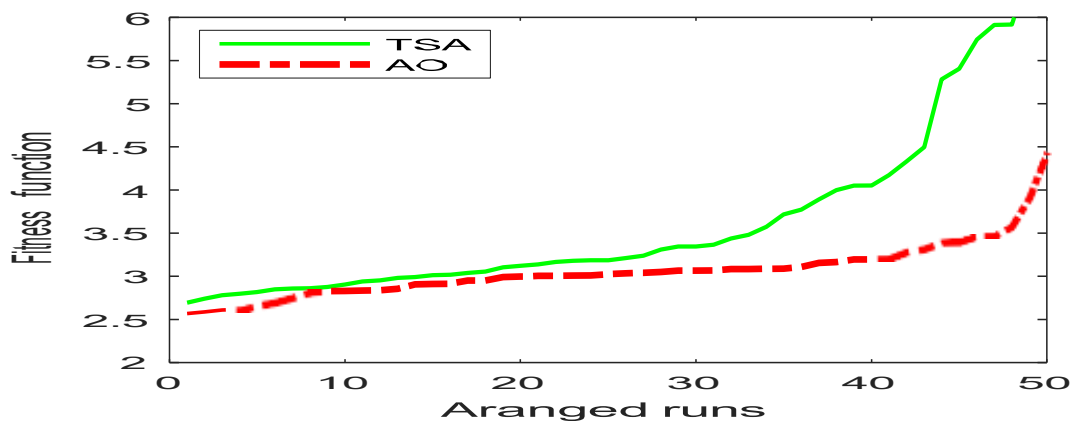


Figure 5. Power loss of 50 trials for Case 2

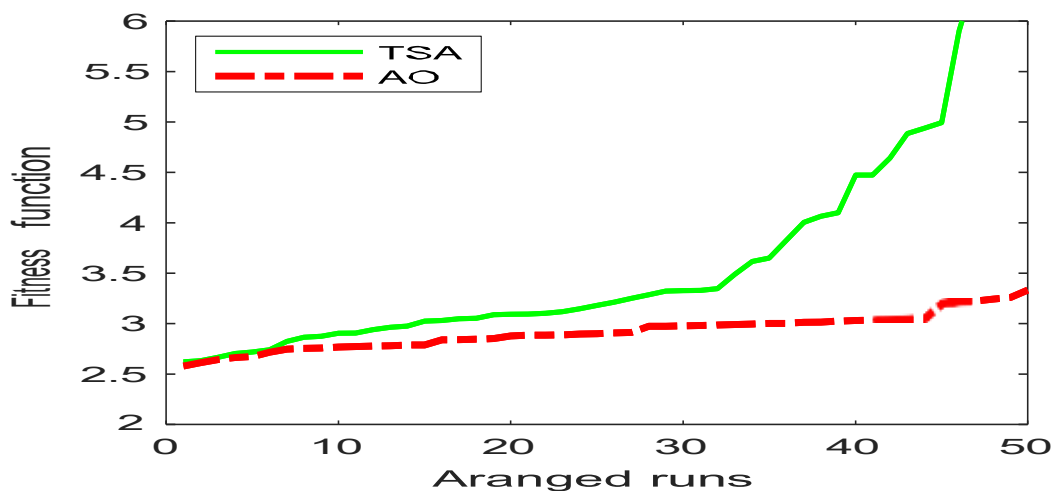


Figure 6. Power loss of 50 trials for Case 3

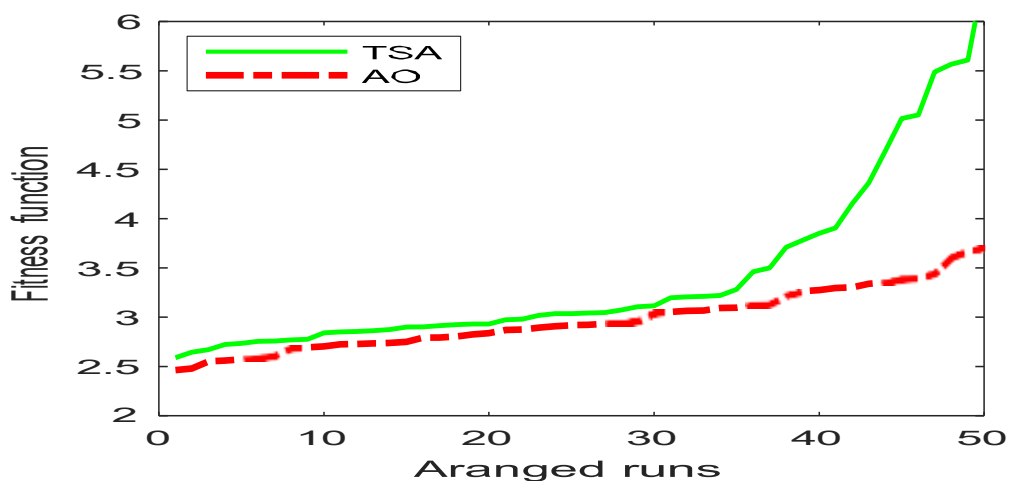


Figure 7. Power loss of 50 trials for Case 4

The best run of 50 trials is also plotted in Figures 8-11. TSA is faster than AO for about one second of the process, but then AO converges to a better solution than TSA for the four cases. Especially, TSA falls into local zones and cannot escape the zones. On the contrary, AO can escape the local zones and get better solutions at the final iteration.

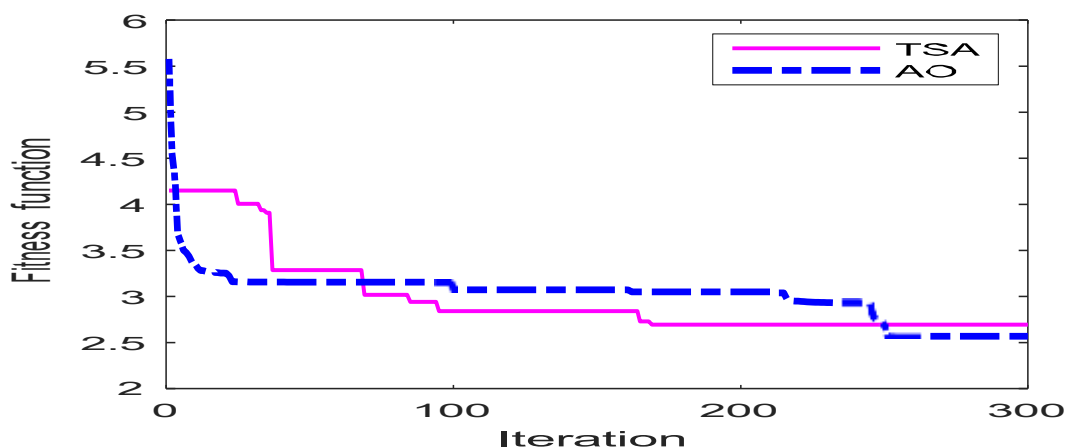


Figure 8. The best run for Case 1

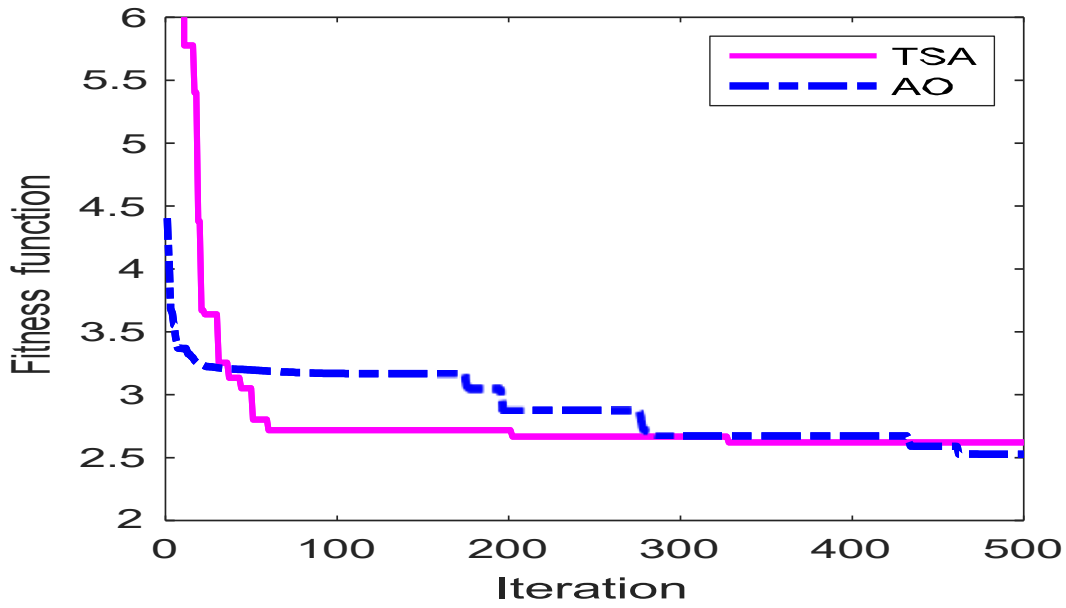


Figure 9. The best run for Case 2

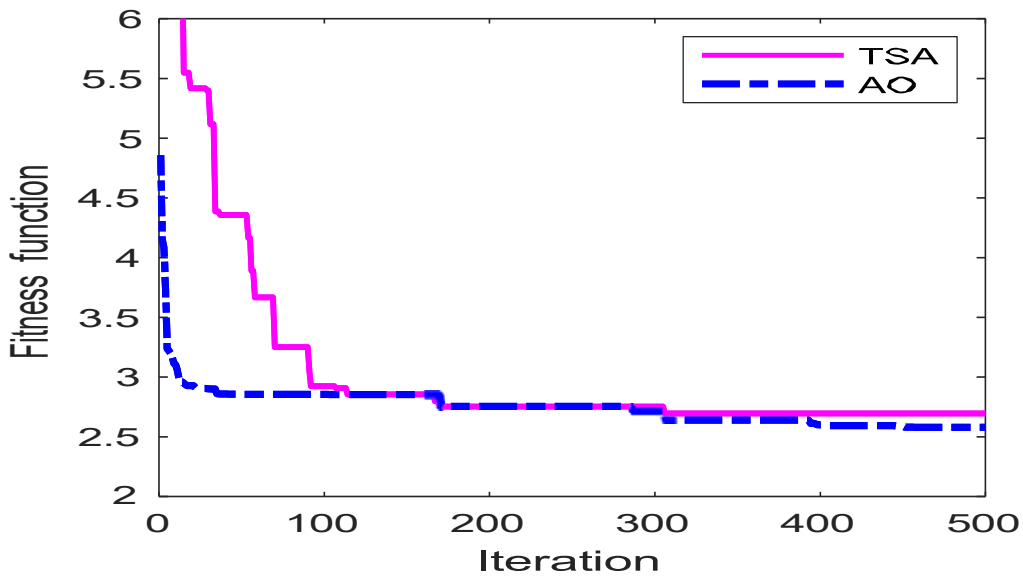


Figure 10. The best run for Case 3

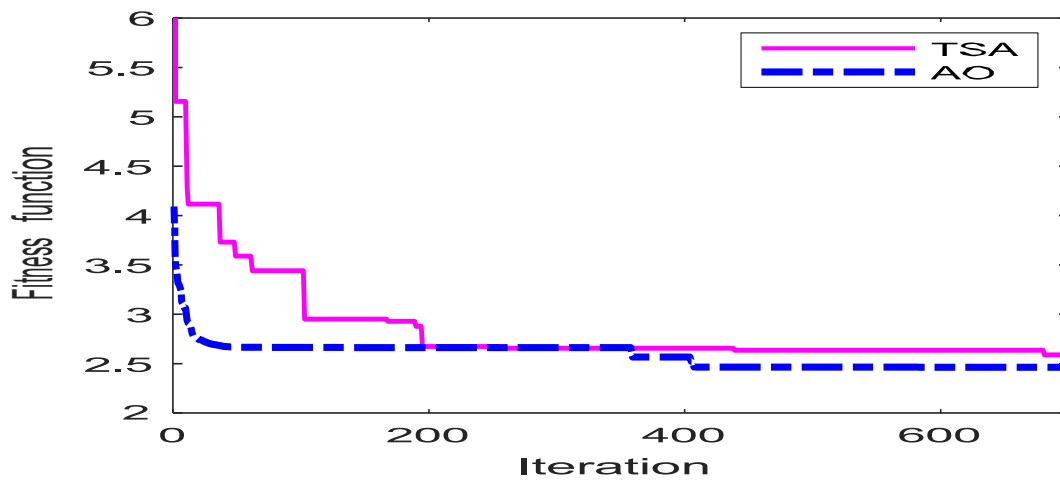


Figure 11. The best run for Case 4

4.3. The improvement of power loss and voltage

The best power loss of AO and TSA is given in Figure 12. TSA's power loss values are 2.693, 2.62, 2.695, and 2.589 MW; meanwhile, those of AO are 2.567, 2.527, 2.58, and 2.463 MW for Cases 1, 2, 3, and 4, respectively. The exact comparisons indicate that the loss of AO is smaller than that of TSA by 4.7%, 3.5%, 4.27%, and 4.87% for the four cases, respectively. The two algorithms find the worst power loss for Case 1 and the best power loss for Case 4. So, this information indicates that using one WPP, one TCSC, and one SVC is the best. The two algorithms have a smaller power loss in Case 2 than in Case 3, so the use of one TCSC is better than one SVC.

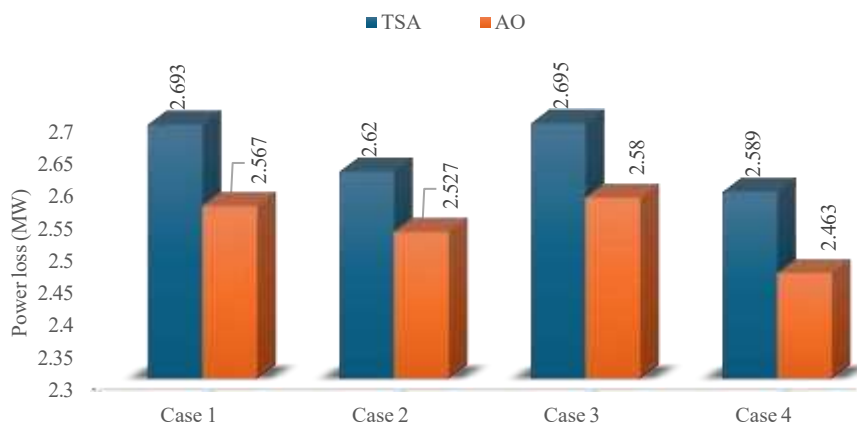


Figure 12. The best loss of each case obtained by TSA and AO

Figure 13 indicates that the voltage profile of Case 4 is the best for buses 13-26; meanwhile, other cases improve voltage from Bus 1 to Bus 9. In general, all buses have a voltage from 1.0 pu to 1.1 pu.

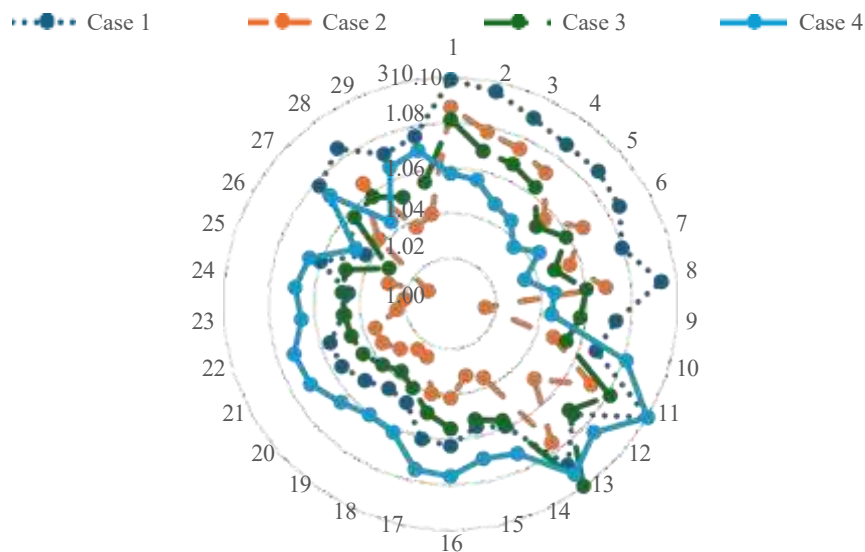


Figure 13. Voltage profile obtained by AO

4.4. Emission of thermal power plants

The emission produced by thermal generating units is reported in Figure 14. The emission of study cases with the installation of wind power plants and FACTS devices do not have a high emission difference; meanwhile, the Base case without FACTS and WPPs has the highest total emission. Case 4, with one 15-MW WPP, one TCSC, and one SVC, owns the smallest emission of 485.56 kg. Compared to Case 1, Case 2, Case 3, and Base Case, the emission is reduced by 1.99, 2.01, 0.92, and 19.68 kg for Case 4. When converting the emission to the cost with the emission price of \$100 per ton, Case 4 can save 0.199, 0.201, 0.092, and 1.968 dollars per hour, compared to Case 1, Case 2, Case 3, and Base Case. If the system's operation lasts 20 years, Case 4 can save $(1.968 \times 8760 \times 20) = 344,829.92$ dollars compared to the Base system without any added components.

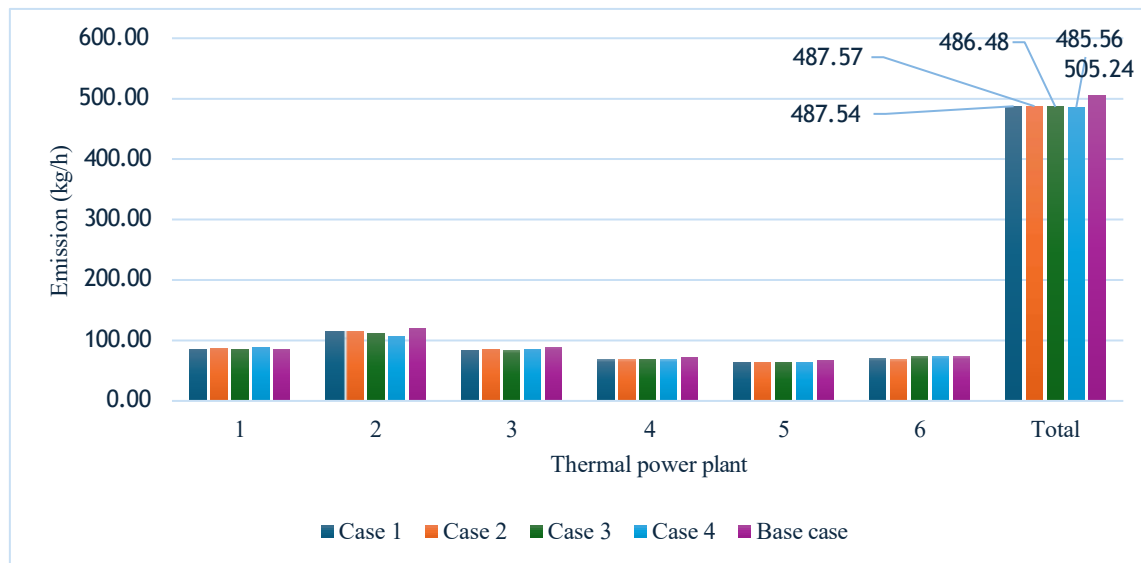


Figure 14. The emission obtained for study cases

V. CONCLUSION

The study optimally installed renewable power plants and FACTS devices in the IEEE 30-bus DPG to minimize power loss. AO and TSA were run for fifty trial runs in four study cases, including Case 1) one 15-MW WPP; Case 2) one 15-MW WPP and one TCSC; Case 3) one 15-MW WPP and one SVC; and Case 4) one 15-MW WPP, one TCSC and one SVC. The results and contributions of the study are as follows:

1. AO could reach better minimum and maximum power loss for the fifty runs than TSA for four cases.
2. AO could find better solutions than TSA at the last 100 iterations; meanwhile, TSA was faster than AO for about one second of the maximum iteration.
3. AO could find smaller losses than TSA by 4.7%, 3.5%, 4.27%, and 4.87% for the four cases, respectively.
4. The two algorithms can find the smallest loss for Case 4 (2.589 MW and 2.463 MW) and the highest loss for Case 1 (2.693 MW and 2.567 MW) among the four cases. Thus, TCSC and SVC are more effective in reducing power loss for the system than in other cases without FACTS or with only one TCSC or one SVC.
5. A huge benefit could be obtained by using FACTS and WPPs. Case 4, with one 15-MW WPP, one TCSC, and one SVC, could reduce emission by 1.99, 2.01, 0.92, and 19.68 kg compared to Case 1, Case 2, Case 3, and Base case. The system, with a 20-year period, could save 344,829.92 dollars compared to the base system, which does not have any added components.

Acknowledgment: This work belongs to the project grant number B2024-SPK-08 funded by Ministry of Education and Training, and hosted by Ho Chi Minh City University of Technology and Education, Vietnam.

REFERENCES

- [1]. Mohammadi, F., & Rashidzadeh, R. (2022). Impact of stealthy false data injection attacks on power flow of power transmission lines—A mathematical verification. *International Journal of Electrical Power & Energy Systems*, 142, 108293.
- [2]. Nguyen, T. T., Vo, D. N., Van Tran, H., & Van Dai, L. (2019). Optimal dispatch of reactive power using modified stochastic fractal search algorithm. *Complexity*, 2019(1), 4670820.
- [3]. Venugopal, S., Asok, P., & Arya, S. R. (2022). Wams-based hierarchical active power differential signal algorithm for backup protection of a facts compensated transmission network. *Advances in Electrical & Electronic Engineering*, 20(4).
- [4]. Dao, T. M., Tran, M. Q., Duong, L. T., Do, D. P. N., Nguyen, N. N., & Vo, D. N. (2024). Temperature dependent optimal power flow using combined particle swarm optimization and differential evolution method. *GMSARN International Journal*, 18(1), 84-105.
- [5]. ALBajaj, B., & Kaplan, O. (2025). Enhanced COVID-19 Optimization Algorithm for Solving Multi-Objective Optimal Power Flow Problems with Uncertain Renewable Energy Sources: A Case Study of the Iraqi High-Voltage Grid. *Energies*, 18(3), 478.
- [6]. Misić, A. S., Karatas, M., & Dasci, A. (2025). Optimal sizing and location of energy storage systems for transmission grids connected to wind farms. *Omega*, 134, 103301.

- [7]. Kiangebeni Lusimbakio, K., Boketsu Lokanga, T., Sedi Nzakuna, P., Paciello, V., Nzuru Nsekere, J. P., & Tshimanga Tshipata, O. (2025). Evaluation of the Impact of Photovoltaic Solar Power Plant Integration into the Grid: A Case Study of the Western Transmission Network in the Democratic Republic of Congo. *Energies*, 18(3), 639.
- [8]. Kedari, S., Veramalla, R., & Kodakkal, A. (2021). Optimized Gains For The Control Of Islanded Solar Photovoltaic And Wind System. *Advances in Electrical & Electronic Engineering*, 19(4).
- [9]. Ullah, Z., Qazi, H. S., Alferidi, A., Alsolami, M., Lami, B., & Hasanien, H. M. (2025). Advanced optimization of renewables and energy storage in power networks using metaheuristic technique with voltage collapse proximity and dynamic thermal rating technology. *Journal of Energy Storage*, 108, 115005.
- [10]. Al-Shetwi, A. Q. (2025). Grid disturbance resilience and stability improvement of grid-connected wind power plants. *Sustainable Energy & Fuels*, 9(4), 1038-1061.
- [11]. Bayat, M., Koushki, M. M., Ghadimi, A. A., Tostado-Véliz, M., & Jurado, F. (2022). Comprehensive enhanced Newton Raphson approach for power flow analysis in droop-controlled islanded AC microgrids. *International Journal of Electrical Power & Energy Systems*, 143, 108493.
- [12]. Hassan, H. A., & Zellagui, M. (2018). Application of grey wolf optimizer algorithm for optimal power flow of two-terminal HVDC transmission system. *Advances in Electrical and Electronic Engineering*, 15(5), 701-712.
- [13]. Pham, L. H., Dinh, B. H., & Nguyen, T. T. (2022). Optimal power flow for an integrated wind-solar-hydro-thermal power system considering uncertainty of wind speed and solar radiation. *Neural computing and applications*, 34(13), 10655-10689.
- [14]. Nguyen, T. T., Nguyen, H. D., & Duong, M. Q. (2023). Optimal power flow solutions for power system considering electric market and renewable energy. *Applied Sciences*, 13(5), 3330.
- [15]. Agrawal, S. P., Jangir, P., Arpita, Pandya, S. B., Parmar, A., Hourani, A. O., ... & Khishe, M. (2025). Exploring the effectiveness of adaptive randomized sine cosine algorithm in wind integrated scenario based power system optimization with FACTS devices. *Scientific Reports*, 15(1), 7090.
- [16]. Chakraborty, S., Maiti, D., Mukhopadhyay, S., Chakrabarti, A., & Biswas, S. K. (2025). Optimized design coordination of a single phase static VAR compensator for AC railway traction. *Electric Power Systems Research*, 243, 111502.
- [17]. Peddiny, V. K., Datta, B., & Banerjee, A. (2025). Performance Improvement of Combined Wind Farms Using ANN-Based STATCOM and Grey Wolf Optimization-Based Tuning. *Journal of Operation and Automation in Power Engineering*, 13(3), 248-254.
- [18]. Kien, L. C., Bich Nga, T. T., Phan, T. M., & Nguyen, T. T. (2022). Coot optimization algorithm for optimal placement of photovoltaic generators in distribution systems considering variation of load and solar radiation. *Mathematical Problems in Engineering*, 2022(1), 2206570.
- [19]. Yuan, C., Zhao, D., Heidari, A. A., Liu, L., Chen, Y., Wu, Z., & Chen, H. (2024). Artemisinin optimization based on malaria therapy: Algorithm and applications to medical image segmentation. *Displays*, 84, 102740.
- [20]. Kaur, S., Awasthi, L. K., Sangal, A. L., & Dhiman, G. (2020). Tunicate Swarm Algorithm: A new bio-inspired based metaheuristic paradigm for global optimization. *Engineering Applications of Artificial Intelligence*, 90, 103541.
- [21]. Basu, M. (2011). Multi-objective optimal power flow with FACTS devices. *Energy Conversion and Management*, 52(2), 903-910.
- [22]. Haddi, S., Bouketir, O., & Bouktir, T. (2018). Improved optimal power flow for a power system incorporating wind power generation by using Grey Wolf Optimizer algorithm. *Advances in Electrical and Electronic Engineering*, 16(4), 471.
- [23]. Nguyen, A. T., Le, C. K., Phan, M. T., & Nguyen, T. T. (2023). Coot Bird Behavior-Based Optimization Algorithm For Optimal Placement Of Thyristor Controlled Series Compensator Devices In Transmission Power Networks. *Advances in Electrical and Electronic Engineering*, 21(3), 171-183.
- [24]. IEEE Standard Systems Data and Single Line Diagrams. Literature-Based Power Flow Test Cases. <http://icseg.iti.illinois.edu/power-cases/> (accessed 15 May 2023).
- [25]. Slimani, L., & Bouktir, T. (2007). Economic power dispatch of power system with pollution control using multiobjective ant colony optimization. *International Journal of Computational Intelligence Research*, 3(2), 145-154.